COMPDYN 2009
ECCOMAS Thematic Conference on
Computational Methods in Structural Dynamics and Earthquake Engineering
M. Papadrakakis, N.D. Lagaros, M. Fragiadakis (eds.)
Rhodes, Greece, 22–24 June 2009

# ESTIMATION OF THE SEISMIC RISK WITH CONSIDERATION OF CAPACITY DEGRADATION OVER TIME

**Daniel Celarec[1], Matjaž Dolšek[2], and Dimitrios Vamvatsikos[3]**

[1,2] University of Ljubljana, Faculty of Civil and Geodetic Engineering
Jamova 2, SI 1000 Ljubljana, Slovenia
e-mail: dcelarec@ikpir.fgg.uni-lj.si, mdolsek@ikpir.fgg.uni-lj.si

[3] University of Cyprus, Department of Civil and Environmental Engineering
Nicosia 1678, Cyprus
e-mail: divamva@ucy.ac.cy

**Keywords:** capacity degradation, corrosion, reinforced concrete, performance-based earthquake engineering, static pushover.

**Abstract.** *The dependence of mankind on the urban built environment is an integral part of culture that is so firmly embedded in our daily life that we are mostly unaware of its existence, as long as functionality is provided. The aging of our structures and the action of natural hazards, such as earthquakes, threaten the functionality of our urban environment and extraordinary expenditures are required to just maintain the status quo. Throughout the world, buildings are reaching the end of their useful life and develop new pathologies that increase their seismic risk, an effect that we aim to capture. In the paper, first, a methodology for structural performance assessment with consideration of capacity degradation over time is presented, utilizing IN2 analysis and an extension of the PEER probabilistic framework to rapidly achieve accurate estimates of limit-state exceedance probabilities of deteriorated structures. In the second part the methodology is applied to an example of a three-storey asymmetric reinforced concrete building. At this stage of the study only an influence of corrosion on longitudinal and transverse reinforcement of the structural elements is considered in the estimation of the seismic risk. The N2 method is used for seismic performance assessment of the structure. It is shown that the capacity in terms of the maximum base shear, as well as in terms of the maximum ground acceleration corresponding to limit states in the nonlinear range, is reduced over time, since the corrosion affects the capacity of both the beams and columns. Consequently, the expected frequency of violating life-safety or near-collapse limit states over the time interval increases in comparison to the typical case where the strength deterioration is neglected.*

## 1 INTRODUCTION

Structures are exposed to aggressive environmental conditions which may cause different types of structural damage. For example, wind, waves, corrosive environment, extreme temperatures and earthquakes are the influences that can impact many existing structures every day. The cycling loads mentioned above can cause corrosion or material fatigue that may lead to the extensive deterioration of mechanical properties of structural elements. Consequently, the structural capacity degrades over time and a lot of economic costs have to be paid just to maintain the serviceability of the structure and to assure the resistance to the loads that such structures were designed for.

Driven by the frequent failures of bridge structures, the influence of corrosion on their traffic load capacity has been widely researched. There, the effects of weathering are more severe since the entire structure is subject to weather conditions. Even for bridges though, most work [1] has focused on the assessment of aseismic structures. Less has been done for structures, especially when under seismic loads, so, we propose to investigate the effect of weathering on the seismic performance of RC structures. This effort becomes especially significant for older, RC-structures designed and constructed in the 1950–1960 era that are nearing the end of their nominal design life. The fundamental understanding of the effect of weathering on our aging infrastructure will help us to get the evidence of the implications of our initial design assumptions on the actual performance of the structures during their entire life, not just when they are still young.

In the present study we are trying to estimate the seismic risk of three-storey asymmetric non-ductile reinforced concrete frame building with consideration of capacity degradation over time. The methodology introduced by Torres and Ruiz [2] is used in analysis, and is based on probabilistic framework proposed by Cornell et al. [3], in addition to which, the structural capacity is considered to changes in time. The structure was modelled using OS Modeler [4] (the sets of Matlab [5] functions) and a nonlinear seismic analysis were performed by employing program OpenSees [6]. In this stage of study only the uniform corrosion along the longitudinal and transverse reinforcement bars of structural elements was considered, which is a simplified approach of modeling the corrosion if compared to more accurate spatial non-homogeneous pitting corrosion [7]. The concrete spalling and reduction of maximum bond stress between concrete and reinforcement bar were not included in the model. That means that corrosion influences only on the diameter of the steel bar. The limit state at structural level was defined independently for ductile and brittle collapse mechanism. It was assumed that the ductile near collapse limit state appears when the maximum strength of structure, in relation to static pushover curve, reduces for 20%, and the brittle near collapse limit state appears if the shear force in the strongest column exceeds its shear strength. The example shows the significant increase in expected frequency of exceedance of brittle near collapse limit if the capacity degradation over time is considered in analysis.

## 2 SUMMARY OF PROBABILISTIC FRAMEWORK

The reliability framework introduced by Torres and Ruiz [2], which was used in this study for structural reliability evaluation considering the capacity degradation over time, is summarized. The summarized framework is straightforward extension of the probabilistic framework proposed by Cornell et al. [3]. In addition to the probabilistic framework introduced by Cornell et al. [3] it is assumed that capacity $C(\tau)$ is random variable with a probability density function $f_C(c|\tau)$ which changes with time. Therefore the conditional probability of failure $P[C(\tau) < S|y,\tau]$ is also a function of time and the expected value of the number of failures during the time interval $(t, t+\Delta t)$ can be expressed as:

$$E\left[n_{F,T}(t,\Delta t)\right]=\int_{t}^{t+\Delta t}\int_{0}^{\infty}\int_{0}^{\infty}P\left[C(\tau)<S\middle|y,\tau\right]f_{C}\left(c\middle|\tau\right)dy\,dc\,d\tau\,. \tag{1}$$

It was shown [2] that the Eq. (1) can be expressed in closed form, similarly as derived by Cornell et al. [3], and can be then written as:

$$\overline{\eta}_{F,T}(t,\Delta t)=k_0(y_{\hat{C}|t})^{-k}\cdot\exp\left[\frac{k^2}{2b_t^2}\left(\sigma_{DR|t}^2+\sigma_{CR|t}^2+\sigma_{DU|t}^2+\sigma_{CU|t}^2\right)\right]\cdot\Omega(t,\Delta t) \tag{2}$$

where $k_0$ and $k$ are the parameters of the hazard curve, $\sigma_{DR|t}$ is the dispersion measure for randomness in displacement demand, $\sigma_{CR|t}$ is the dispersion measure for randomness in displacement capacity, $\sigma_{DU|t}$ and $\sigma_{CU|t}$ are, respectively, the dispersion measure for uncertainty in displacement demand and capacity, and $b_t$ is the parameter of the relationship between the seismic intensity measure and engineering demand parameter (e.g. displacement). The seismic intensity measure $y_{\hat{C}|t}$ is related to the limit state capacity $\hat{C}(t)$ at the beginning of the evaluation time interval:

$$y_{\hat{C}|t}=\left(\frac{\hat{C}(t)}{a_t}\right)^{\frac{1}{b_t}} \tag{3}$$

and

$$\Omega(t,\Delta t)=\frac{(\alpha+\beta t)}{\beta}\frac{b_t}{(b_t-k)}\left[\left(1+\frac{\beta\Delta t}{\alpha+\beta t}\right)^{1-\frac{k}{b_t}}-1\right]. \tag{4}$$

The simplified expression of Eq. (1) is based on several assumptions. The hazard curve has to be approximated around the $y_{\hat{C}|t}$ and the relationship between the seismic intensity measure and the engineering demand parameter has to be fitted around the $\hat{C}(t)$ by the following power-law expressions:

$$\nu(y)=k_0y^{-k},\ \ \hat{D}(t)=a_ty^{b_t}\,. \tag{5}$$

The median capacity $\hat{C}(\tau)$ is assumed to vary linearly with time:

$$C(t)=\alpha+\beta\cdot t,\ \alpha>0 \text{ and } \beta\le 0\,. \tag{6}$$

In addition it is assumed that all dispersion measures and the parameters of the relationship between the seismic intensity measure and the engineering demand parameter ($a_t$, $b_t$) are constant over the integration time interval $\Delta t$. The demand $D$ and capacity $C(t)$ are assumed to be lognormally distributed. The dispersion measures related to demand and capacity are therefore defined as standard deviation of logarithm of the demand and capacity, respectively.

In our case the probabilistic framework is applied for probabilistic seismic performance assessment of the structure. Therefore determination of the relationship between the seismic intensity measure and the engineering demand parameter may become extremely time-consuming if the engineering demand parameter is determined with nonlinear dynamic analysis, which has to be performed for several intensity measures and different ground motion records in order to capture randomness due to earthquakes, e.g. with incremental dynamic analysis [8]. In addition, analyses have to be performed also for selected ages/milestones during the design life of the structure. Therefore, for practical application, simplified analysis methods become very attractive. In our study the relationship between the seismic intensity measure and the engineering demand parameter, which changes with time (age of structure), was determined with the incremental N2 analysis (IN2) [9,10], which is a

The global result of the IN2 analysis is an IN2 curve, which represents the "mean estimate" of the engineering demand parameter given the seismic intensity measure, and it is intended to approximate a summarized (i.e., mean) IDA curve. The procedure for determination of the IN2 curve is explained elsewhere [10]. For common structural systems with moderate or long fundamental period(s) IN2 curve results in a straight line. In this case the "equal displacement rule" applies, i.e. $b_t$=1.0 (Equation 5), up to the "failure" point, which is conservatively represented by the near collapse limit state. After "failure", the IN2 curve becomes a horizontal line. In more general cases, the IN2 curve can be determined in the same way as in the case of IDA, i.e. from two points of the actual curve, e.g. from the points representing the damage limitation and near collapse limit states, or by regression over the whole curve.

Since the IN2 curve is only a mean result, it does not contain any dispersion information. Therefore the dispersion measures for randomness in displacement demand $\sigma_{DR|t}$ and displacement capacity $\sigma_{CR|t}$ cannot be determined from such results. Still, we can use existing results from other works [10],[11], who have found that the coefficient of variation for the displacement of SDOF systems varied from 0,4 for structures with a moderate or long natural period, to 0,7 for structures with a short predominant period.

The determination of dispersion measures for uncertainty in displacement demand $\sigma_{DU|t}$ and capacity $\sigma_{CU|t}$ is in general possible to determine with the IN2 method, but requires a probabilistic structural model, i.e. a model with appropriate consideration of parameter uncertainties, which is not within the scope of this paper. However, it is convenient to predetermine the dispersion measures for uncertainty even if the relationship between seismic intensity measure and engineering demand parameter is determined with incremental dynamic analysis. For example, dispersions for steel frames have been proposed in the FEMA-350 Guidelines [12]. They may serve as rough estimates also for some other structural systems. For example, the total uncertainty dispersion measure $\sigma_{UT} = (\sigma_{DU}^2 + \sigma_{CU}^2)^{0.5} = 0.35$ was applied for a global inter-story drift evaluation in the case of low-rise buildings within the SAC-FEMA seismic performance evaluation [13].

## 3 EXAMPLE OF THE THREE-STOREY REINFORCED FRAME

### 3.1 Description of the structure

The example structure is a three-storey asymmetric reinforced concrete frame building. This structure was pseudo-dynamically tested within a SPEAR project (M. Fardis and P. Negro, coordinators) and analysed in previous studies [14]. The elevation, the plan of the building and the reinforcement in typical cross sections of the columns and beams are shown in Figure 1. The structure was designed for gravity loads only.

### 3.2 The structural model

The columns and beams of the structure were modelled by one-component lumped plasticity elements, which consist of an elastic beam/column element and two inelastic rotational hinges at the ends, defined by a moment-rotation relationship. These relationships were determined for the columns by properly taking into account their axial load and its interaction with the moment capacity. Gravity loads for this RC structure amounted to 6,3 kN/m$^2$ and 6,2 kN/m$^2$ for first two stories and top storey, respectively. A schematic moment-rotation envelope is shown in Figure 2.

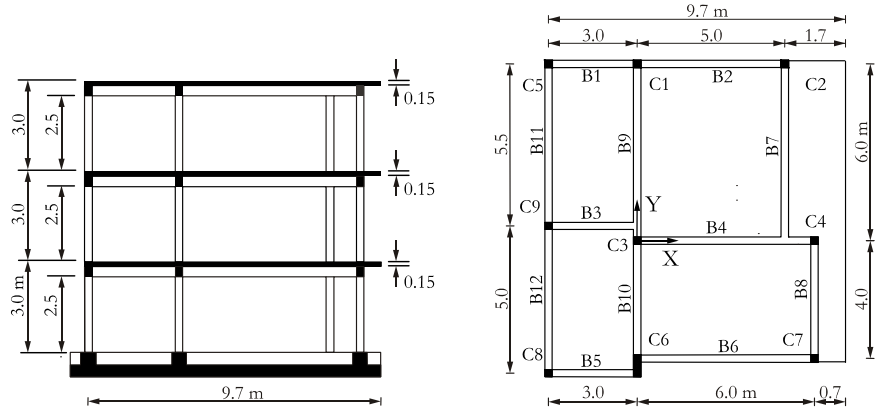


a) the elevation and the plan view of the SPEAR building

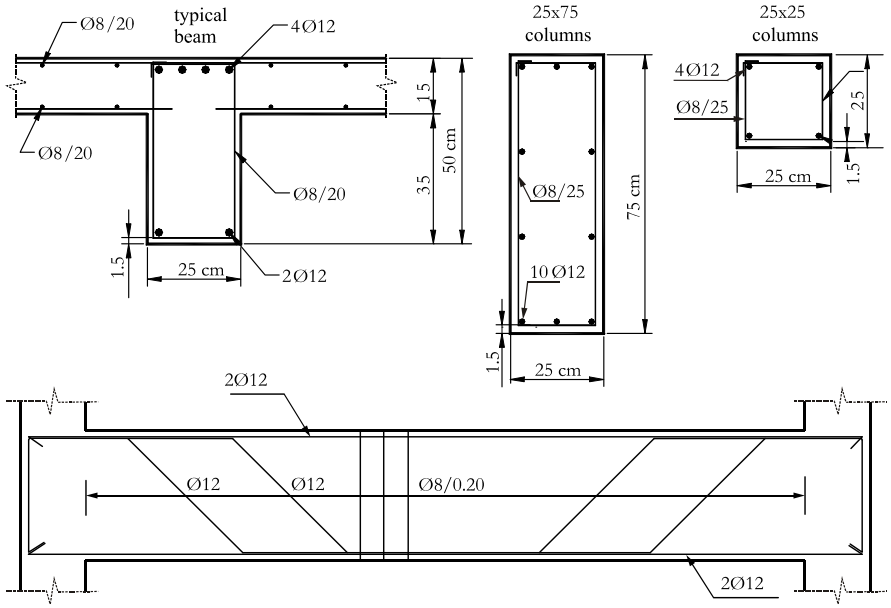


b) typical reinforcement in beams and columns

Figure 1: a) The elevation and plan view of example structure, and b) the typical cross-sections and reinforcement in columns and beams.

Rigid diaphragms were assumed at the floor levels due to monolithic RC slabs. Consequently the masses and mass moments of inertia were lumped at the mass centres. The masses and the mass moments of inertia amounted to 65,5 t and 1196 tm$^2$ for the first two stories, and 64,1 t and 1254 tm$^2$ for the top storey, respectively. The centreline dimensions of the elements were used with the exception of beams which are connected eccentrically to the column C6. Using centreline dimensions, the storey heights of 2,75 and 3,0 m, respectively, for the first and upper two storeys, were assumed.

The yield and maximum moment of the moment-rotation envelope was determined from appropriate section analysis. The characteristic rotations, which describe the moment-rotation envelope of a plastic hinge, were determined according to the procedure described by Fajfar et al. [14]. The zero moment point was assumed to be at the mid-span of the columns and beams. Therefore the rotations $\theta_y$ for moment-rotation envelopes of columns and beams were calculated using the formula:

$$\theta_y = \frac{M_Y \cdot l_{span}}{6 \cdot E \cdot I_{eff}}, \tag{7}$$

where $l_{span}$ is the length of a beam or column, $E$ is the modulus of elasticity and $I_{eff}$ is the effective moment of inertia of the element (0,5 $I$).

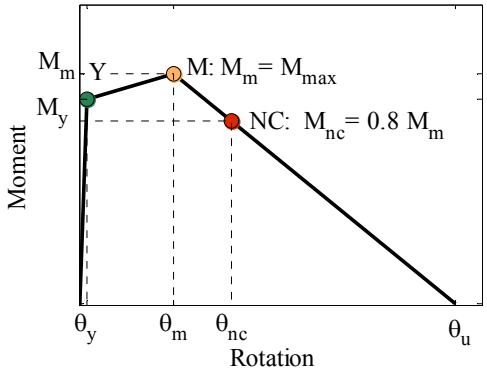


Figure 2: Schematic moment-rotation relationship of a plastic hinge in columns and beams**.**

The ultimate rotation $\theta_{u,c}$ in the columns, which corresponds to a 20% reduction in the maximum moment, was estimated by means of the Conditional Average Estimate (CAE) method [15], whereas the ultimate rotation for hinges in beams $\theta_{u,b}$ were determined using the formula defined in [16]:

$$\theta_{u,b} = \frac{1}{\gamma_{el}} 0,016 \cdot (0,3^{\nu}) \cdot \left[ \frac{\max(0,01;\omega')}{\max(0,01;\omega)} f_c \right]^{0.225} \cdot \left( \frac{L_V}{h} \right)^{0.35} \cdot 25^{\left( \alpha \rho_{sx} \frac{f_{yw}}{f_c} \right)} \cdot (1.25^{100\rho_d}) . \qquad (8)$$

where $\gamma_{el}$ is equal to 1,0 (mean values as for secondary elements), parameter $v$ is the normalised axial load (for beams: $v$=0), $\omega$ and $\omega'$ are the mechanical reinforcement ratios of the tension and compression longitudinal reinforcement, $f_{cm}$ and $f_{yw}$ are the mean strength of concrete (MPa) and yield strength of steel (MPa), respectively, $\rho_{sx}$ is the ratio of transverse steel parallel to the direction of loading, $\rho_d$ is the steel ratio of diagonal reinforcement in each diagonal direction and $\alpha$ is the confinement effectiveness factor. All beams are defined as members without detailing for earthquake resistance. Therefore the rotations at near collapse limit state $\theta_{nc}$ are multiplied by 0,825. The post-capping or negative-stiffness part of moment-rotation envelope is determined considering the assumption that ratio between the ultimate rotation $\theta_{u,b}$ and rotation at maximum moment $\theta_{m,b}$ is 3,5. Schematic moment-rotation relationship of a plastic hinge in columns and beams is shown on Figure 2.

The degradation of capacity over time was modelled only with the simplified model of corrosion of longitudinal and transverse reinforcement in the external (i.e. exposed) elements of the structure. In general, the corrosion decreases the diameter of reinforcement and the bond stress between the concrete and steel bars. The later phenomenon and as well as spalling of concrete were not considered in this stage of the study. Therefore in our model the corrosion influences only the diameter of the steel bar. The reduced diameter $D_{rb}(t)$ of a reinforcing steel bar with initial diameter of $D_b$ (mm), which is subjected to corrosion for a time period (years) $\Delta t = t - t_0$ ($t_0$ represents corrosion initiation time in years) is according to [17]:

$$D_{rb} = D_b - 0,023 i_{corr} \Delta t \text{ (mm)}, \qquad (9)$$

where $i_{corr}$ represent the mean annual corrosion current per unit anodic surface area off steel ($\mu A/cm^2$). In our analysis the corrosion current $i_{corr}$=1,2 $\mu A/cm^2$ was considered, which corresponds to a high level of reinforcement corrosion exposure [17].

In order to determine the structural capacity as linear function of time, six deterministic models $M_0$, $M_{10}$, $M_{20}$, $M_{30}$, $M_{40}$ and $M_{50}$ for time periods: 0, 10, 20, 30, 40 and 50 years after construction of the structure were generated. For example, the moment-rotation envelopes for column C5 and beam B1 (Figure 1) in the first storey for different time periods are presented on Figure 3. The first free modal periods of undamaged structure are: $T_X$=0,80 s $T_Y$=0,67 s and $T_{RZ}$=0,538 s. The period $T_2$ and corresponding mode shape, which is the most important for seismic performance assessment of the structure in Y direction, were used in the N2 method (Section 3.5).

### 3.3 Definition of limit state and nonlinear static analyses

The frequency of exceedance was determined for a brittle and ductile near collapse limit state. According to European standard [16] the near collapse (NC) limit state at the element level is defined with the ultimate rotation of plastic hinge (e.g Eq. (8)), which corresponds to 20% drop of moment (Figure 3) and is related to ductile collapse mechanism, and with the shear strength, which is related to brittle collapse mechanism. The shear strength of element was calculated according to [16]:

$$V_R = \frac{1}{\gamma_{el}}\left[\frac{h-x}{2L_V}\min\left(N;0,55A_c f_c\right)+\left(1-0,05\min\left(5;\mu_\Delta^{pl}\right)\right)\right]\cdot \left[0,16\max\left(0,5;100\rho_{TOT}\right)\left(1-0,16\min\left(5;\frac{L_V}{h}\right)\right)\sqrt{f_c}A_c+V_W\right], \tag{10}$$

where $\gamma_{el}$ was assumed 1,0 in order to get the mean value of the shear strength, $h$ is the depth of cross-section, $x$ is the compressive axial force, $L_v$ is the ratio moment/shear ($M/V$), $A_c$ is the cross-section area calculated as $b_w d$, $f_c$ is the concrete compressive strength, $\rho_{tot}$ is the total longitudinal reinforcement ratio and $V_w$ is the contribution of transverse reinforcement to shear resistance, taken as equal to:

$$V_w = \rho_w \cdot b_w \cdot z f_{yw}. \tag{11}$$

The limit state at structural level was defined independently for the ductile and brittle collapse mechanism. Since the limit state at structural level is not defined in the standard it was assumed that the ductile near collapse limit state appears when the maximum strength of structure, in relation to static pushover curve, reduces for 20% (limit state A), and the brittle near collapse limit state appears if the shear force in the strong column C6 (Figure 1) exceeds its shear strength. Limit states A and B are denoted on Figure 4.

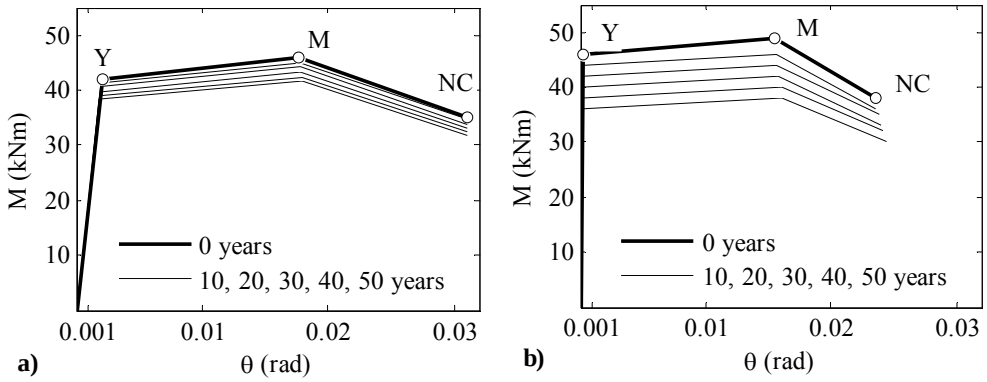


Figure 3: The moment-rotation envelopes for (a) column C5 and (b) beam B1 in the first storey considering capacity degradation over time.

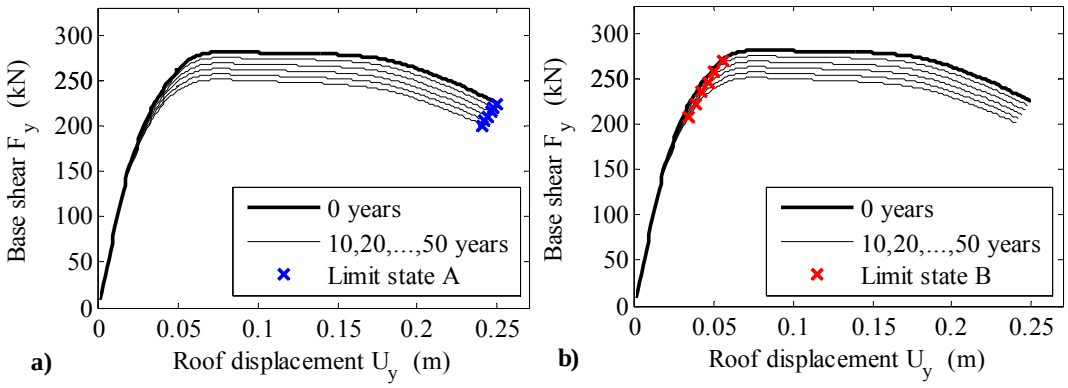


Figure 4: The pushover curves for different time periods and near collapse points at (a) limit state A and (b) limit state B.

In general nonlinear static analysis is performed independently in X and Y direction. For brevity, results are presented only for pushover analysis in Y direction of the global coordinate system that is in the direction of strong side of column C6 (Figure 1). The influence of the unsymmetrical plan of the structure on the results of analyses is practical negligible. The imposed horizontal loads were determined by the product of storey masses and modal shape [9], which are presented later in Section 3.5. Displacement of structure was monitored at mass centre at the top of the building.

The nonlinear static (pushover) analyses were performed for the structure at time (age) 0, 10, 20, 30, 40 and 50 years. The pushover curves for models $M_0$, $M_{10}$, $M_{20}$, $M_{30}$, $M_{40}$ and $M_{50}$ corresponding to different time periods (age of structure) are presented in Figure 4. The values for maximum load resistance $F_{max}$ and displacements $D_{nc}$ at limit state A and limit state B are outlined in Table 1.

The shear strength versus weight ratio is 11% for the new structure (time 0) and decreases during aging process. After 50 years the strength of the structure is reduced for about 13,3%. The difference in the top displacement in limit state A due to ageing of the structure is not so important as the difference in the strength of the structure (it amounts to 3,6%) since area of the longitudinal reinforcement does not have an important influence on the ultimate rotation in plastic hinges (Figure 3), whereas the top displacement in limit state B is significantly reduced (about 38 %).

| Model label | Time $t$ (y) | Max. load $F_{max}$ (kN) | Limit state A $d_{nc}$ (m) | Limit state B $d_{nc}$ (m) |
|---|---|---|---|---|
| $M_0$ | 0 | 284 | 0,250 | 0,055 |
| $M_{10}$ | 10 | 276 | 0,248 | 0,050 |
| $M_{20}$ | 20 | 268 | 0,246 | 0,046 |
| $M_{30}$ | 30 | 261 | 0,244 | 0,042 |
| $M_{40}$ | 40 | 254 | 0,242 | 0,038 |
| $M_{50}$ | 50 | 246 (-13%) | 0,241 (-3,6%) | 0,034 (-38%) |

Table 1: The values for maximum load resistance $F_{max}$ and displacements $D_{nc}$ for limit states A and B.

### 3.4 The elastic response spectrum and the seismic hazard curve

In the study the seismic hazard curve for the South-East part of Slovenia [18] was used and it was idealized with function $H(s)=k_0 \times s^{-k}$, where $k$ and $k_0$ are the parameters of the hazard function [3]. In the idealization procedure the intervals from 0,25 $a_{g,nc}(t_0)$ to 1,25 $a_{g,nc}(t_{50})$ were selected [18], where $a_{g,nc}(t_0)$ is the peak ground acceleration for undamaged structure

$k$=3,275, $k_0$=5,280×10$^{-6}$ for limit state A

and

$k$=1,300, $k_0$=3,260×10$^{-6}$ for limit state B.

The seismic load is defined with the elastic response spectrum according to European standard [19] for a soil class C. The seismic hazard curve for a peak ground acceleration and elastic response spectrum are presented on Figure 5. The intensities for return periods 225, 475 and 2475 years as well as maximum ground accelerations for limit states A and B are marked on the curve. Note that the peak ground acceleration was selected for intensity measure.

### 3.5 The maximum ground acceleration at different age of structure

The peak maximum ground acceleration ($a_{g,nc}$) was determined by the N2 method [9]. The process of determination of $a_{g,nc}$ is explicitly presented for limit state A for model $M_0$ while for other age of structure and for limit state B only the results are presented.

The pushover curve has to be idealized as shown in Figure 6a in order to determine quantities of the single degree of freedom model (SDOF). The results of idealization are the yield force $F_y$ and yield displacement $D_y$. The quantities of the SDOF system are determined by dividing the quantities of the MDOF system by the transformation factor Γ:

$$\Gamma = \frac{m_{SDOF}}{\sum m_i \cdot \phi_i^2} = 1,27;\ m_{SDOF} = \sum m_i \cdot \phi_i = 128,6 \text{ t}, \tag{12}$$

where $m_{SDOF}$ is the mass of SDOF system, $m$={65,6 65,6 64,1} t is a vector of storey masses and $\phi_Y$={0,25 0,70 1.00} is the mode shape vector of the predominant translational mode shape in Y direction. Yield point of the SDOF system is obtained simply as $d_y = D_y/\Gamma = 0,034$ m and $f_y = F_y/\Gamma = 224$ kN. The period of the SDOF system is calculated as follows:

$$T_{SDOF} = 2 \cdot \pi \cdot \sqrt{\frac{m_{SDOF} \cdot d_y}{f_y}} = 0,870 \text{ s}. \tag{13}$$

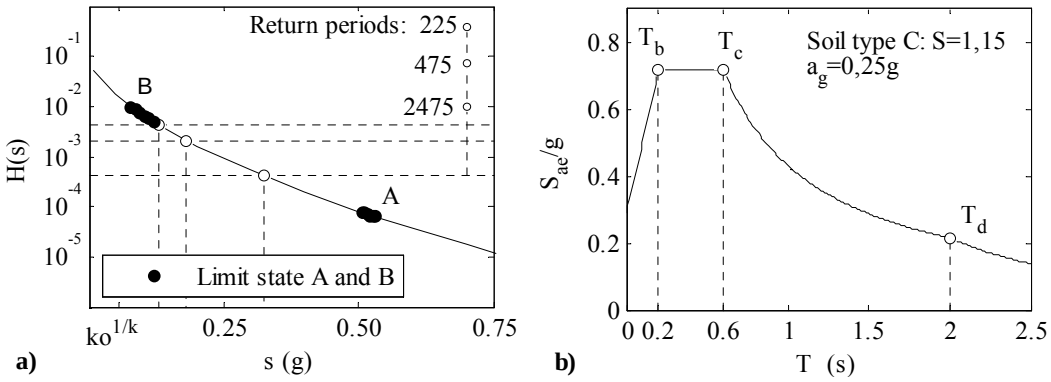


Figure 5: a) The function of seismic hazard and b) elastic response spectrum according to EN 1998-1 for soil type C.

The periods of all equivalent SDOF systems are obviously within the medium-period range of the spectrum (Figure 5) and exceed the characteristic period $T_C$, which is the corner period between the constant acceleration and constant velocity ranges in an idealized Newmark-Hall type spectrum. The equal displacement rule can therefore be applied for the determination of spectral acceleration, which corresponds to the NC limit state. Therefore the $S_{ae,nc}$ is:

$$S_{ae,nc} = d_m \cdot \left( \frac{2 \cdot \pi}{T_{SDOF}} \right)^2 = 10,3 \; m/s^2 \tag{14}$$

and peak acceleration $a_{g,nc}$ corresponding to the NC limit state is determined from the elastic spectrum as follows:

$$a_{g,nc} = \frac{S_{ae,nc}(T_{SDOF})}{S \cdot \eta \cdot 2,5} \cdot \frac{T_{SDOF}}{T_C} = 5,20 \text{ m/s}^2 = 0,530 \text{ g} . \tag{15}$$

The presented evaluation of the $a_{g,nc}$ is shown also in AD format together with the capacity diagram of the SDOF system (Figure 6b).The procedure for determination of the maximum ground acceleration, which corresponds to the NC limit state, was repeated for limit state B and for other selected age of structure. The results for ground accelerations $a_{g,nc}$ are outlined in Table 2. The reduction in maximum ground acceleration $a_{g,nc}$ is similar to that shown before for the maximum top displacement (Section 3.3, Table 1) and is about 4,7% for limit state A and 34% for limit state B.

### 3.6 Structure capacity in terms of maximum top displacements as function of time

The structure capacity is defined in terms of maximum top displacement corresponding to the NC limit states defined in Section 3.3 and varies linearly in time: $C(t)=\alpha+\beta \times t$. The parameters $\alpha$ and $\beta$ that defines linear function $C(t)$ are calculated using linear regression (i.e. the method of least squares). The values are:

$$\alpha = 0,2499 \text{ and } \beta = 0,0002 \rightarrow \text{for limit state A,}$$
$$\alpha = 0,0548 \text{ and } \beta = 0,0004 \rightarrow \text{for limit state B.}$$

The top displacements corresponding to defined limit states and ages/milestones of structures are presented in Figure 7a and 7b, respectively, for limit state A and B. The fitted lines approximate the decrease of median capacity over structural lifetime. The values of fitted top displacements $d_{nc,fitt}$ and corresponding maximum ground accelerations $a_{g,nc}$ for limit states A and B are presented in Table 2. Note, that top displacements $d_{nc,fitt}$ in Table 2 are values fitted with linear function and are different from those in Table 1.

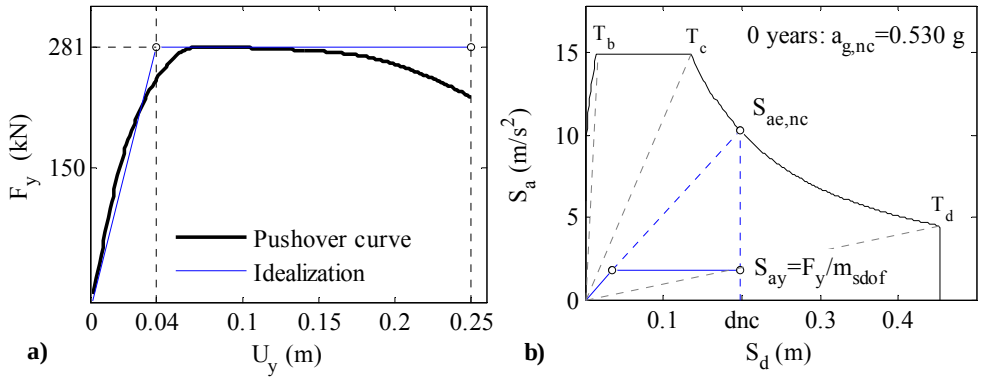


Figure 6: a) Idealization of pushover curve for model $M_0$ and b) the AD format for SDOF sistem.

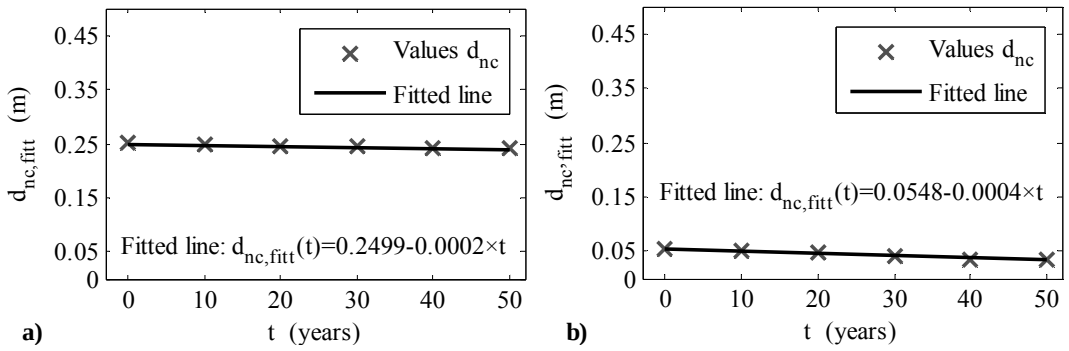


Figure 7: The values for maximum top displacement at predefined age of structure and fitted line that approximate structure capacity as function of time for a) limit state A and b) limit state B.

| Time (years) | Limit state A | | Limit state B | |
|---|---|---|---|---|
| | $d_{nc,fitt}$ (m) | $a_{g,nc}$ (m/s$^2$) | $d_{nc,fitt}$ (m) | $a_{g,nc}$ (m/s$^2$) |
| 0 | 0,249 | 0,530 | 0,055 | 0,119 |
| 10 | 0,248 | 0,525 | 0,051 | 0,109 |
| 20 | 0,246 | 0,521 | 0,047 | 0,102 |
| 30 | 0,244 | 0,516 | 0,043 | 0,094 |
| 40 | 0,242 | 0,510 | 0,039 | 0,085 |
| 50 | 0,240 | 0,507 | 0,035 | 0,077 |

Table 2: The expected number of failures $\eta_{FT}$ for NC limit states A and limit state B.

### 3.7 Expected number of failures over lifetime of the structure

The expected number of exceedance of NC limit state $\eta_{F,T}$ for different age of structure were calculated by means of Eq. (2), where the initial conditions correspond to time $t$=0 years and the time increments $\Delta t$ = 10, 20, 30, 40 and 50 years were considered. The seismic hazard $H(a_{g,c})$ was defined with the seismic hazard curve for the South-East part of Slovenia [18] (Section 3.4) and dispersions for randomness in seismic demand and capacity were considered to be equal to 0,4 and 0,2, respectively. Dispersions for uncertainty in displacement demand and capacity were assumed equal to 0,25. In addition also the annual frequency of exceedance of NC limit state was calculated. The expression for annual frequency of exceedance of NC limit state is:

$$\overline{\eta}_{F,T}(t,1) = H(a_{g,nc|t}) \cdot e^{\frac{k^2}{2b_t^2}\left(\sigma^2_{DR|t}+\sigma^2_{CR|t}+\sigma^2_{DU|t}+\sigma^2_{CU|t}\right)} \tag{16}$$

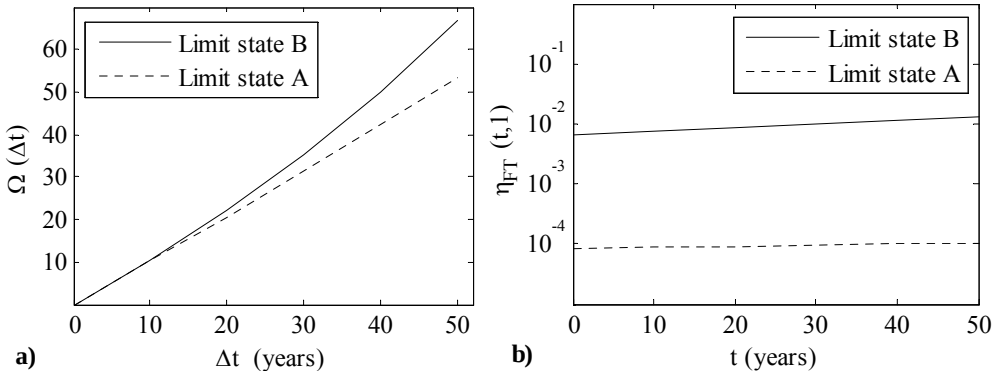


Figure 8: a) The factor $\Omega$ ($t$) and b) annual frequency of exceedance $\overline{\eta}_{F,T}(t,1)$ for limit states A and B.

The factor $\Omega(t)$ and annual frequency $\overline{\eta}_{F,T}(t,1)$ are shown in Figure 8 and the expected number of exceedance of NC limit state $\eta_{F,T}$ for different periods are presented in Figure 9.

If degradation of structural capacity is neglected, the expected number of failures over the time interval ($t$, $\Delta t$) was evaluated considering the assumption that parameter $\beta$, that controls the capacity degradation gradient, is equal to 0. In that case the limit of parameter $\Omega$:

$$\lim_{\beta \to 0} \Omega(t, \Delta t) = \Delta t \tag{17}$$

The expected number of exceedance of NC limit state B in time interval (0, 50 years) is 0,437 and it is 33 % higher than in the case where the degradation was not considered. For limit state A the difference is not so important, it amounts to 7,1 %. The values for both limit states and for different time periods are presented in Figure 9 and Table 3. The continuous curve represents the expected numbers of failures considering the capacity degradation over time and the dashed curve represents the case when the degradation was neglected. The picture 9a and 9b are related to limit state A and limit state B, respectively.

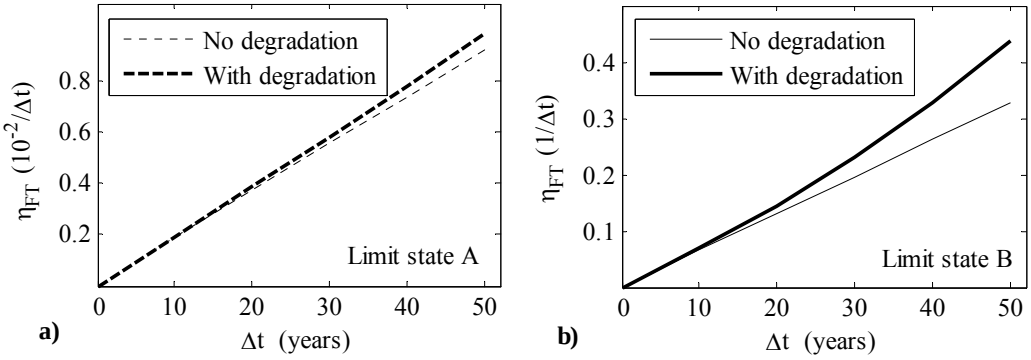


Figure 9: The expected number of failures $\eta_{FT}$ for (a) NC limit state A and (b) NC limit state B for different periods of design structure life.

| Time (years) | Limit state A: $\eta_{FT}(1/\Delta t)$ | | Limit state B: $\eta_{FT}(1/\Delta t)$ | |
|---|---|---|---|---|
| | Degradation | | Degradation | |
| | Yes | No | Yes | No |
| 10 | 0,004 | 0,004 | 0,069 | 0,066 |
| 20 | 0,008 | 0,007 | 0,145 | 0,131 |
| 30 | 0,012 | 0,011 | 0,230 | 0,197 |
| 40 | 0,016 | 0,015 | 0,327 | 0,262 |
| 50 | 0,020 | 0,018 | 0,437 | 0,328 |

Table 3: The expected number of failures $\eta_{FT}$ for NC limit state A and B presented for different periods of design structure life.

## 4 CONCLUSIONS

A simplified methodology has been presented for estimating the seismic performance of aged RC structures. Considering only the deterioration of longitudinal and shear reinforcement due to corrosion, and utilizing simplified analysis techniques within a SAC/FEMA-like probabilistic framework [20], we are able to estimate the changing mean annual frequency of limit-state exceedance as it worsens with time. Finally, the total probability of limit-state exceedance is quantified over the design life of the structure, providing us with a cumulative single measure of the structure's performance as aging sets in.

In our case-study of a 3-story non-ductile RC structure, corrosion is shown to only slightly influence the moment capacity of beams and columns, while their shear capacity was heavily degraded. We observed a 33 % increase in the probability of collapse over the lifetime of the building, a significant increase that simply cannot be ignored. It is envisaged that further refinement of our techniques with inclusion of concrete spalling and bond degradation will only worsen such conclusions. Thus, further verification of such results is needed in order to better understand the actual risks faced by our aging infrastructure and appropriately amend our design codes.

## ACKNOWLEDGMENT

The authors wish to acknowledge the financial support provided by the Cyprus Research Promotion Foundation and Slovenian Research Agency under research grants SLO-CY/407/04 and BI-CY/08-09-002, respectively.

## REFERENCES

[1] A.C. Estes, D.M. Frangopol, Bridge lifetime system reliability under multiple limit states, ASCE Journal of Bridge Engineering 6(6): 523-528, 2001.

[2] M.A. Torres, S.E. Ruiz, Structural reliability evaluation considering capacity degradation over time, *Engineering Structures,* **29**, 2183-2192, 2007.

[3] C.A. Cornell, F. Jalayer, R.O. Hamburger, D.A. Foutch, Probabilistic Basis for 2000 SAC Federal Emergency Management Agency Steel Moment Frame Guidelines, *Journal of Structural Engineering*, **128**, 526-533, 2002.

[4] M Dolšek, OSmodeler User's Manual, Version 1, University of Ljubljana, 2008

[5] MathWorks, Matlab R2007a.

http://www.mathworks.com/products/matlab

[6] F. McKenna F, G.L. Fenves, Open system for earthquake engineering simulation, Pacific Earthquake Engineering Research Center, Berkeley, California, 2004. http://opensees.berkeley.edu/

[7] Mark G. Stewart, Mechanical behaviour of pitting corrosion of flexural and shear reinforcement and its effect on structural reliability of corroding RC beams. *Structural safety,* **31**:19-30, 2009.

[8] D. Vamvatsikos, C.A Cornell, Incremental Dynamic Analysis. *Earthquake Engineering and Structural Dynamics*; **31**:491-514, 2002.

[9] P. Fajfar, A nonlinear analysis method for performance-based seismic design. *Earthquake Spectra*, **16**(3):573-592, 2000.

[10] M. Dolšek, P. Fajfar, Simplified probabilistic seismic performance assessment of plan-asymmetric buildings. *Earthquake Engineering and Structural Dynamics*, **36**:2021–2041, 2007.

[11] J. Ruiz-Garcia, E. Miranda (2003), Inelastic displacement ratios for evaluation of existing structures, *Earthquake Engineering and Structural Dynamics*, **32**:1237-1258, 2003.

[12] FEMA 350, *Recommended seismic design criteria for new steel moment frame buildings*, SAC Joint Venture, Federal Emergency Management Agency, Washington (DC), 2000.

[13] S-Y. Yun, R.O. Hamburger, C.A. Cornell, D.A. Foutch, Seismic performance evaluation for steel moment frames. *Journal of Structural Engineering ASCE*; **128**(4):534-545, 2002.

[14] P. Fajfar, M. Dolšek, D. Marušić, A. Stratan, Pre- and post-test mathematical modeling of a plan-asymmetric reinforced concrete frame buildings. *Earthquake Engineering and Structural Dynamics*, **35**:1359-1379, 2006.

[15] I. Peruš, K. Poljanšek, P. Fajfar, Flexural deformation capacity of rectangular RC columns determined by the CAE method. *Earthquake Engineering and Structural Dynamics*, **35**:1453-1470, 2006.

[16] CEN. Eurocode 8: Design of structures for earthquake resistance. Part 3: Strengthening and repair of buildings. *EN 1998-3*, European Committee for Standardisation, Brussels, March 2005.

[17] S.J. Pantazopoulou, K.D. Papoulia, Modeling Cover-Cracking due to Reinforcement Corrosion in RC Structures J. *Engrg. Mech*. **127**(4):342-351, 2001.

[18] M. Dolšek, P. Fajfar, The effect of masonry infills on the seismic response of a four storey reinforced concrete frame–a probabilistic assessment. *Engineering Structures,* **30**:3186-3192, 2008.

[19] CEN. Eurocode 8: Design of structures for earthquake resistance. Part 1: General rules, seismic actions and rules for buildings, EN 1998-1. CEN, Brussels, December 2004.

[20] Cornell CA, Jalayer F, Hamburger RO, Foutch DA. The probabilistic basis for the 2000 SAC/FEMA steel moment frame guidelines. *ASCE Journal of Structural Engineering* 2002; 128(4):526-533.